Flexible phosphor films doped with Mie resonators for enhanced out-coupling of the emission

ELECTRONIC SUPPLEMENTARY INFORMATION

José M. Miranda-Muñoz, Dongling Geng, Mauricio E. Calvo, Gabriel Lozano, and Hernán Míguez.

- Total reflectance, total transmittance and absorptance spectrum of 4-µm nanophosphor films:

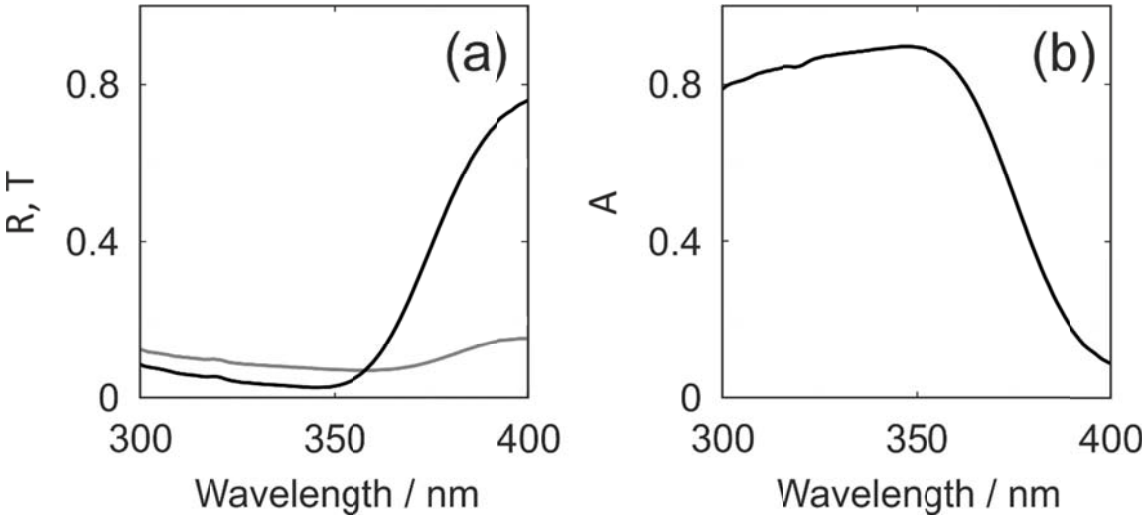

Figure S1. (a) Spectral total reflectance, R, (grey curve) and total transmittance, T, (black curve) of a 4-µm nanophosphor film on a quartz substrate. (b) Absorptance spectrum, A, of the same system yielded from the spectra in (a) as 1 – R – T.

Maximized absorptance, defined as A = 1 – R – T, where R is the total reflectance and T the total transmittance of the nanophosphor film on a quartz substrate, is desired around the pumping wavelength, λ_{pump} = 365 nm. To that aim, a study of the effect of the thickness of the nanophosphor film on the value of such magnitude around the pumping wavelength was performed, concluding that around 4-µm thickness was enough to absorb up to 76% of the incident light at 365 nm, as illustrated in Figure S1(b). The correspondent R and T curves are displayed in Figure S1(a). A quartz substrate was employed in order to avoid any absorption component at the substrate.

- Fabrication of luminescent films with Dy^{3+}-doped nanophosphors:

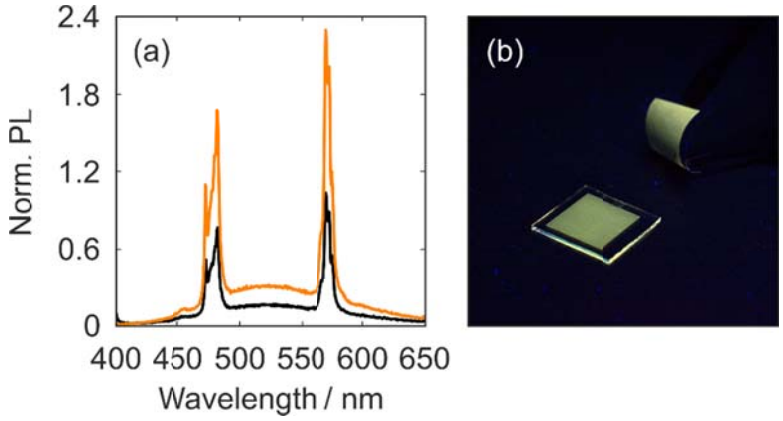

Figure S2. (a) Photoluminescence spectra under irradiation at λ_{pump} = 352 nm for a 4-µm layer based on $GdVO_4$:Bi^{3+},Dy^{3+} nanophosphors with (orange curve) and without (black curve) the incorporation of spherical TiO_2 scattering centres. (b) Rigid (down-left) and flexible (up-right) luminescent films based on Dy^{3+}-doped nanophosphors. Thickness is around 4 µm.

One of the main advantages of the developed layer fabrication process is its generality, which enables the use of nanophosphors doped with other rare earth elements when seeking different emission properties. Here, we employed $GdVO_4$ matrices doped with Bi^{3+} and Dy^{3+}, $GdVO_4$:Bi^{3+},Dy^{3+}, yielding films presenting yellowish photoluminescence. Therefore, following the procedure described in the main manuscript for the fabrication of films from a suspension of phosphors, we were able to develop films with and without spherical TiO_2 inclusions as scattering centres. As displayed in Figure S2(a), the integration of scattering centres causes a PL enhancement when compared to a bare matrix, in the same way that Eu^{3+}-doped nanophosphors. The improved extraction of the emitted light is evidenced by the reduction of light guided escaping through the edges of the substrate, as shown in Figure 4(f) in the main manuscript. Eventually, the experimental procedure allows release of the layer, yielding a high-quality flexible film displaying intense emission, Figure S2(b).

- Spherical TiO2 scattering centres:

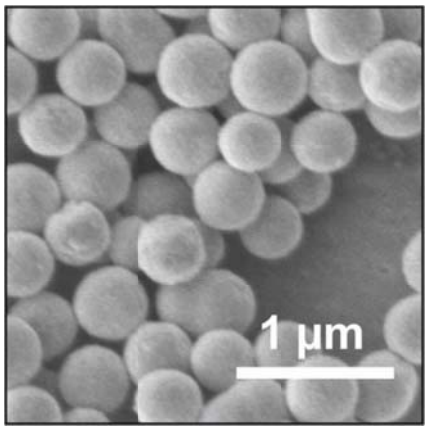

Figure S3. Scanning Electron Microscopy (SEM) image of the crystalline TiO_2 spheres used as scattering centres for the integration of optical disorder in the luminescent nanophosphor-based matrices. The average size of the spheres is r = (225 ± 20) nm.

- Optical constants employed in the calculations of the l_{sc} spectra by means of Mie formalism:

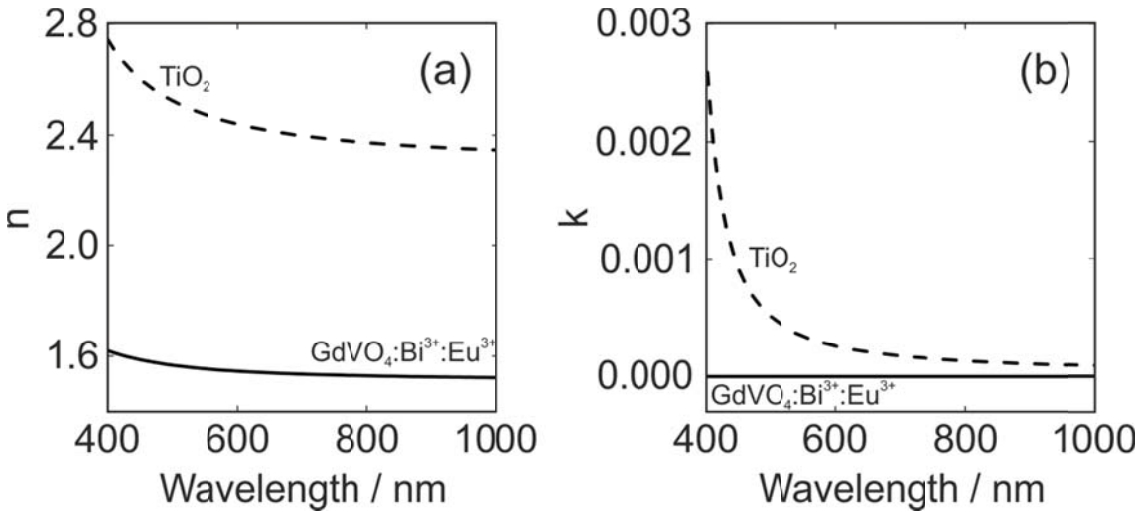

Figure S4. Spectral refractive index (a) and extinction coefficient (b) of the nanophosphors and the TiO_2 spheres employed in the calculations of the scattering mean free path, l_{sc}, performed using Mie formalism.

- Conservation of the emission properties from rigid to flexible film:

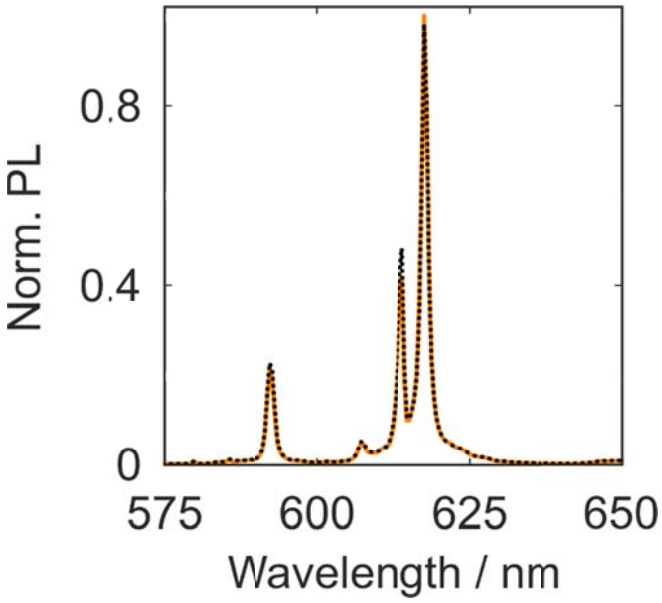

Figure S5. (a) Photoluminescence spectra under irradiation at λ_{pump} = 365 nm for a 4-µm PMMA-infiltrated layer based on $GdVO_4:Bi^{3+},Eu^{3+}$ nanophosphors before (black-dotted curve) and after (orange curve) layer release.

Figure S5 demonstrates that the PL spectrum of the films is not significantly modified after layer release. Thus, since the emission properties hardly change from the rigid to the flexible material, the study of the effect of optical disorder on the modification of the luminescent properties has been wholly performed on rigid layers in order to reduce experimental difficulty.

- Time-dependent photoluminescence fittings:

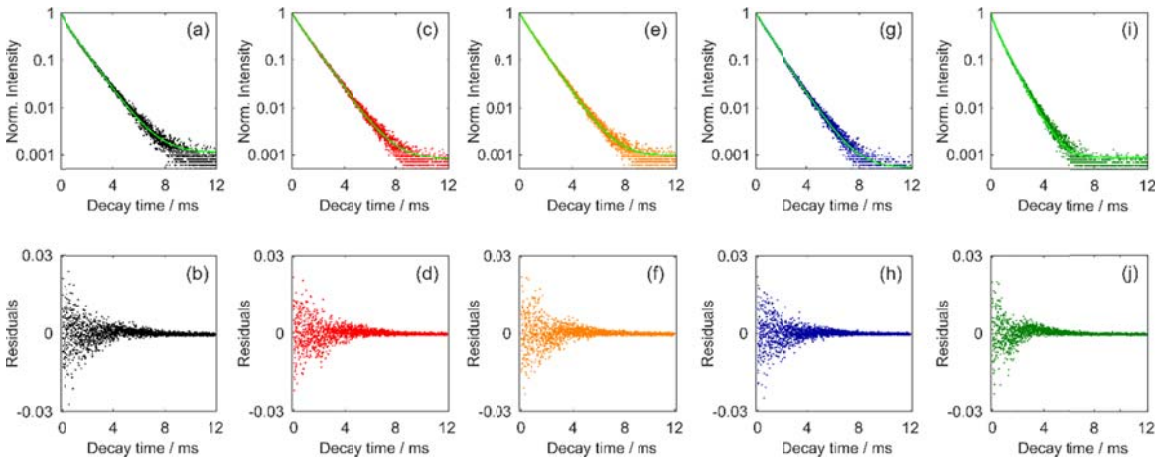

Figure S6. Time-resolved PL decay curves of the Eu^{3+} cations along with the curves (light-green) resulting from their fitting to a double exponential model (upper row) and their correspondent residuals (lower row). The data presented refer to a reference sample (a-b), and samples incorporating spherical TiO_2 scattering centres with 5% (c-d), 10% (e-f), 12% (g-h) and 15% (i-j) concentrations.

- Excitation of the nanophosphor layers by LED radiation:

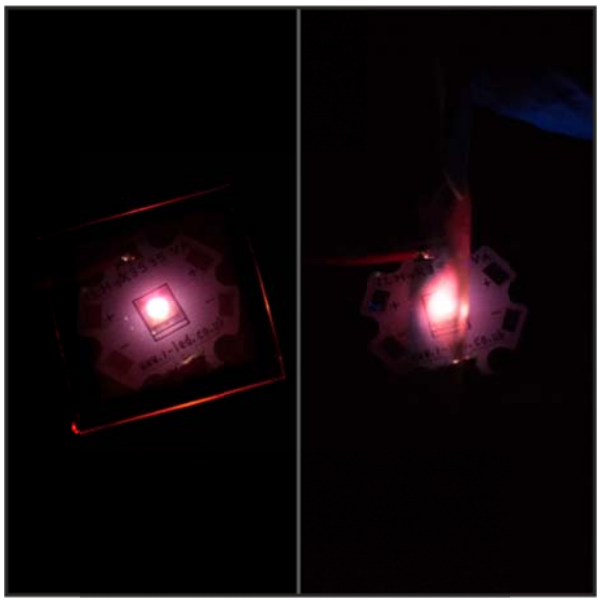

Figure S7. Luminescent rigid (left) and flexible (right) bare nanophosphor layer under LED excitation at λ = 380 nm.

We proceeded to test the suitability of these conversion layers for integration into emitting devices. Explicitly, the material was shone with radiation from an LED emitting at λ = 380 nm and red emission was revealed. Figure S7 illustrates this observation for a reference layer, confirming that both versions of the conversion layer, rigid and solid, are susceptible to operate, displaying red photoluminescence, under UVA-LED irradiation.

- Thermal stability of the flexible emitting layers:

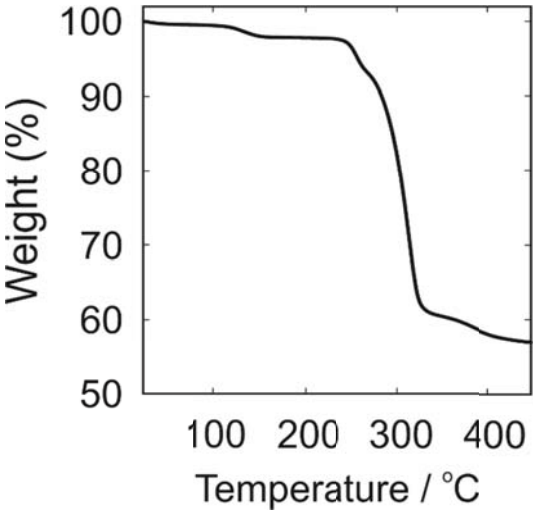

Figure S8. Thermal gravimetric analysis (TGA) performed on a flexible emitting nanophosphor-based layer supported on PMMA.

The nanophosphors presented in the main manuscript are known to possess excellent thermal stability. For that reason, layers herein prepared employing this material are expected to preserve such feature. A different situation rises in the case the emitting layer is embedded in another material. The flexible layers fabricated in this work are encapsulated in PMMA and their thermal stability are then highly dependent on that of this polymeric support. Indeed, the TGA curve displayed in Figure S8 indicate that the thermal stability of the flexible layer is dictated by that of the PMMA, which remains stable up to 250^{o}C, thus proving its suitability for LED integration.